Received December 1, 2019, accepted December 22, 2019, date of publication December 27, 2019, date of current version January 24, 2020.

Digital Object Identifier 10.1109/ACCESS.2019.2962716

Low-Profile Beamforming-Network-Avoiding Multi-Beam Antenna Based on Parasitic Patch and Shorting-Pin

ZEKUI ZHANG[1,2], WENMEI ZHANG[1], YUFENG LIU[1], RUNBO MA[1], AND LIPING HAN[1]
[1]School of Physics and Electronic Engineering, Shanxi University, Taiyuan 030006, China
[2]No.33 Research Institute of China Electronics Technology Group Corporation, Taiyuan 030006, China

Corresponding author: Wenmei Zhang (zhangwm@sxu.edu.cn)

This work was supported in part by the National Science Foundation of China under Grant 61771295 and Grant 61775126, in part by the Excellent Achievement Cultivation Project for Universities in Shanxi Province under Grant 2019KJ001, in part by the Shanxi 1331 Project Key Subjects Construction under Grant 1331KSC, and in part by the National Science Foundation of Shanxi Province under Grant 201901D111025.

ABSTRACT In this paper, a new method to design multi-beam antenna based on parasitic patch and shorting-pin is proposed and demonstrated through two cases of single- and multi-source. For the single-source multi-beam antenna, by arranging the parasitic patch shorted with pins around a square patch, the beam is divided into four parts and a multi-beam radiation is realized. Also, arc slots in the parasitic patch are added to improve the bandwidth and shorting-pins located along the edges of square patch are introduced to adjust the operating frequency, gain and pitch angle. The multi-source multi-beam antenna has a similar construction with the single-source case except it has four ports. In addition, an asymmetric gap is added in the square patch to improve the isolation between the four ports. Finally, both the simulated and measured results verify the proposed methodology. The realized single-source antenna operates in the range of 5.22 - 5.42 GHz. Four beams point at $(\varphi, \theta) = (0°, 41°)$, $(90°, 35°)$, $(180°, 41°)$ and $(270°, 38°)$. For the multi-source case, the corresponding bandwidth is 5.25 - 5.48 GHz. The radiation beams are steered to $(\varphi, \theta) = (0°, 30°)$, $(270°, 37°)$, $(90°, 30°)$ and $(180°, 37°)$.

INDEX TERMS Multi-beam, parasitic patch, port isolation, shorting-pin.

I. INTRODUCTION

The multiple beam antennas have been widely applied in mobile communication networks, multiple-target radar systems and satellite communications [1]. Normally, there are two methods to produce multiple beams. One is using reflector [2]–[4], and the other is using beamforming network (BFN) and radiating array [5]–[7]. The former controls electromagnetic wave according to the focusing and reflection characteristics. For the latter, BFNs usually consist of Blass matrixes or Butler matrixes formed by power dividers, directional couplers and phase shifters.

In recent years, some novel multi-beam antennas based on metasurface with a low profile have been reported [8]–[11]. In [8], a method to control electromagnetic (EM) radiation by holographic metasurfaces was proposed. Also, a combined theory of holography and leaky wave to realize the multi-beam radiation was presented. In [9], a parallel-plate waveguide (PPW) holographic metasurface antenna capable of producing dual-polarized multi-beam radiation pattern was demonstrated. Furthermore, in [12]–[14], some shared aperture metasurface antennas with multiple ports were proposed. Besides, a dipole electrically steerable parasitic array radiator (ESPAR) antenna that can be applied to multi-input-multi-output communication was suggested [15], [16].

On the other hand, shorting-pins were used to control the operating frequency and the radiation pattern of microstrip antennas [17], [18].

In this paper, a new type of multi-beam antenna avoiding beam-forming network is presented. By arranging shorted parasitic patches around a square patch, the corresponding current distribution is optimized and radiation beam is divided into four parts. In addition, for single-source antenna, shorting-pins along the edge of square patch are introduced to adjust the operating frequency, gain and pitch angle. With regard to multi-source antenna, the isolations between two

The associate editor coordinating the review of this manuscript and approving it for publication was Kai-Da Xu.

ports are improved by etching an asymmetric gap in the square patch. In Section II and Section III, the design concept, theory and radiation characteristics of the proposed antennas are presented in greater detail. In Section IV, measured results are presented to validate the effectiveness of the method. Finally, conclusion is drawn in Section V.

II. DESIGN OF THE SINGLE- SOURCE MULTI-BEAM ANTENNA

The proposed single-source multi-beam antenna consists of a patch layer on one side of dielectric substrate that has a ground plane in other side. The used substrate is Rogers 5880 with relative permittivity of 2.2 and loss tangent of 0.0009. Figure 1 shows the structure of the patch layer. It comprises of a square patch and four parasitic patches. The square patch is shorted at each edge with five shorting-pins of radius $r = 0.5$ mm. For four parasitic patches, a shorting-pin with radius $r_s = 0.5$ mm is placed near the edge of patch. Also, an arc slot with a width $d = 0.8$ mm and inner radius $r_1 = 14$ mm is introduced. The designed antenna operates at 5.3 GHz and optimized dimensions are summarized in Table 1.

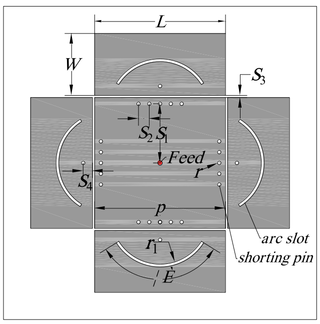

FIGURE 1. Structure of the patch layer.

TABLE 1. Summary of single-source antenna geometry.

Symbol	p	L	W	S_1	S_2	S_3	S_4	θ
Value (mm)	37.6	37.6	17.8	17	3.1	0.6	2.7	116°

A. PRINCIPLE OF FORMING MULTIPLE BEAMS

In order to form multiple beams, four parasitic patches are placed around a square patch. Also, each parasitic patch is shorted by a shorting-pin. Therefore, radiation aperture is divided into four parts and four beams are realized. This working principle can be revealed by analyzing the vector current distribution and the radiation pattern of three antennas as shown in Figures 2 and 3. As can be seen in Figure 2(a), not in its fundamental mode, square patch works in its TM_{20} and TM_{02} mode. In this case, the radiation pattern as shown in Figure 3(a) can be observed. In Figure 2(b), after the shorting-pins are placed at the edge of square patch, the current distribution is similar to Figure 2(a) except that in the middle of every edge is enhanced a little. Therefore, in Figure 3(b), the radiation level along the diagonal is enhanced. Finally, after four parasitic patches shorted with a shorting-pin are added as shown in Figure 2(c), strong induced current is generated in the parasitic patches. As can be seen, the parasitic patches operate in its TM_{20} mode instead of fundamental mode. As a result, the beam is separated into four parts with a gain of 7.26 dBi as shown in Figure 3(c) and the pitch angle of each beam is 47°.

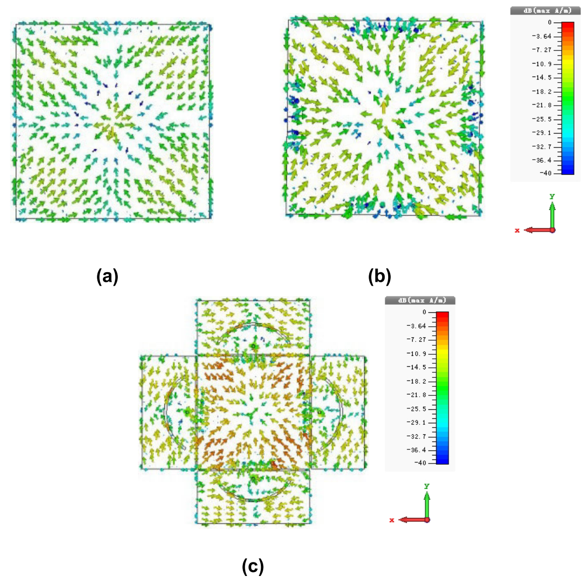

FIGURE 2. Surface currents distribution at 5.3 GHz. (a) Only a square patch; (b) Square patch is shorted with shorting-pins; (c) Adding parasitic patches shorted with shorting-pins.

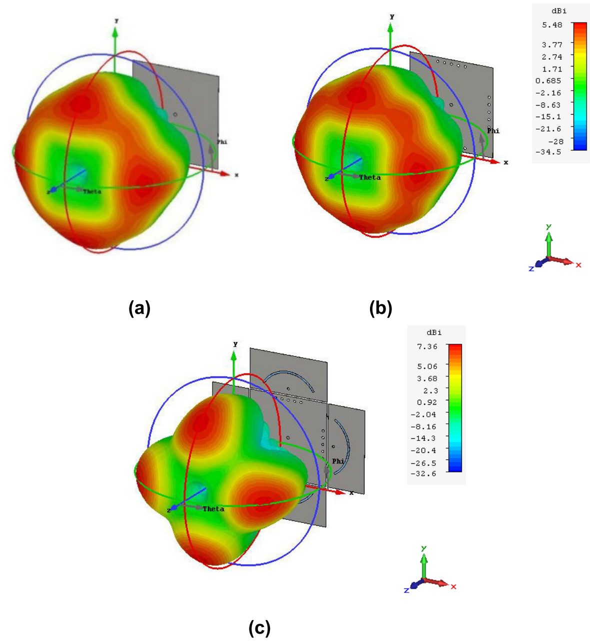

FIGURE 3. Simulated radiation patterns of the single-source antenna at 5.3GHz: (a) Only a square patch; (b) Square patch is shorted with shorting-pins; (c) Adding parasitic patches shorted with shorting-pins.

B. INFLUENCE OF SHORTING-PIN IN THE SQUARE PATCH

The shorting-pins between the square patch and the ground plane are mainly used to adjust the resonant frequency, gain

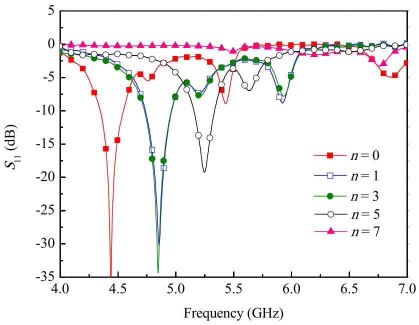

FIGURE 4. S_{11} **for different number of shorting-pins.**

TABLE 2. Antenna performance for different *n*.

Number (n)	Resonant Frequency (GHz)	θ	Gain (dBi)
0	4.44	40°	4.49
1	4.86	34°	5.06
3	4.85	34°	5.07
5	5.30	47°	7.36
7	6.67	21°	6.97

and pitch angle. This can be observed in Figure 4 and Table 2. Figure 4 shows the S_{11} for different number of shorting-pin (n). It indicates that the antenna operates at 4.4 GHz when there is no shorting-pin. When n increases from 1 to 5, the operating frequency rises from 4.8 to 5.3 GHz. Increasing it to 7 continuously, the impedance matching becomes very bad. Table 2 presents gain and pitch angle θ when n is changed. It indicates, as n increases from 1 to 5, the gain gradually increases and θ varies between 34° and 47°. While in case of $n = 7$, gain and θ are all reduced. As a result, $n = 5$ is selected to obtain an appropriate working frequency, high gain and large pitch angle.

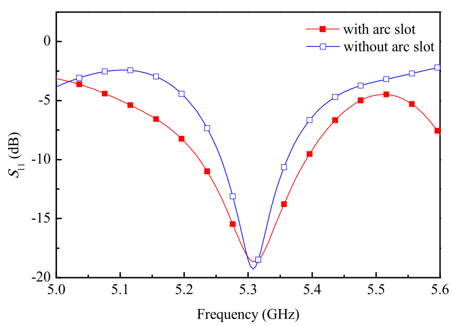

FIGURE 5. **Simulated** S_{11} **with and without arc slot.**

C. INFLUENCE OF ARC SLOT IN THE PARASITIC PATCH

The arc slots in the parasitic patches are mainly used to improve the bandwidth and they have less influence on the radiation pattern. Figure 5 shows the S_{11} with and without arc slots. It can be observed that the antenna can operate from 5.26 to 5.36 GHz when there is no arc slot. However, after the arc slots are etched, the impedance bandwidth ($S_{11} < -10$ dB) increases to 170 MHz (from 5.22 GHz to 5.39 GHz) because the current paths for different frequency are provided by the arc slots.

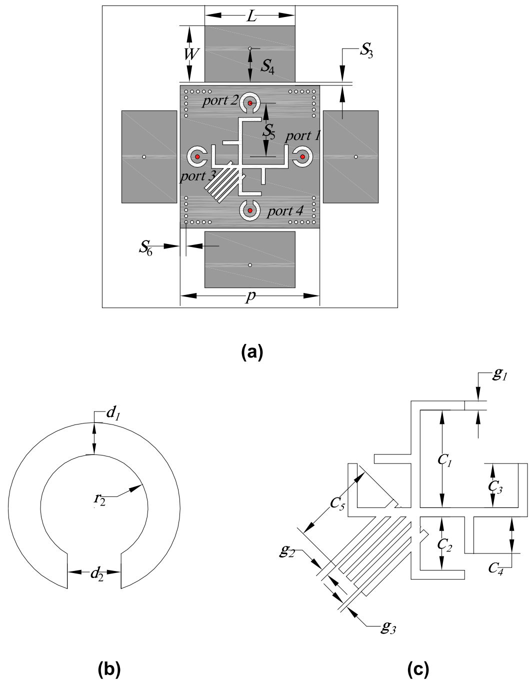

FIGURE 6. Patch layer of the proposed multi-source multi-beam antenna. (a) Final configuration. (b) Open ring. (c) Asymmetric gap.

III. DESIGN OF THE MULTI-SOURCE MULTI-BEAM ANTENNA

Unlike single-source multi-beam antennas, the multi-source multi-beam antenna consists of four ports, called ports 1-4, and the geometry of its patch layer is shown in Figure 6(a). Also, around every port, an open ring (shown in Figure 6(b)) is etched to adjust the impedance matching of the antenna. In addition, in order to improve the isolation between the four ports, an asymmetric gap, as shown in Figure 6(c), is introduced in the square patch. The structural parameters of the multi-source multi-beam antenna are given in Table 3.

TABLE 3. Summary of multi-source antenna geometry.

Symbol	p	L	W	S_3	S_4	S_5	S_6	r_2	d_1
Value (mm)	42.5	27.5	16.8	1.0	10	16	1.8	2.0	1.2
Symbol	d_2	C_1	C_2	C_3	C_4	C_5	g_1	g_2	g_3
Value (mm)	2.0	12.8	7	5.8	4.8	11.5	1.2	0.9	0.5

A. WORKING MECHANISM OF MULTI-SOURCE MULTI-BEAM ANTENNA

For the multi-source case, the principle of forming multiple beams is similar to that of single source. It can be investigated through the current distribution. Considering the symmetry of antenna structure, only the cases when ports 1 and 4 are excited are provided. Figure 7 shows the results at 5.3 GHz for port 1. In Figure 7(a), the current mainly concentrates near the parasitic patch closing to port 1 and its direction is parallel to the short side of the parasitic patch. As a result, a beam shown in Figure 7(b) having a maximum level at $(\varphi, \theta) = (0°, 30°)$ is formed. Its polarization direction is along x-axis. The corresponding results when port 4 is excited are shown in Figure 8. Differing from the Figure 7(a), the current in Figure 8(a) flows along the -y-axis, thus forming a polarized wave along -y-axis. The maximum radiation appears at $(\varphi, \theta) = (270°, 37°)$.

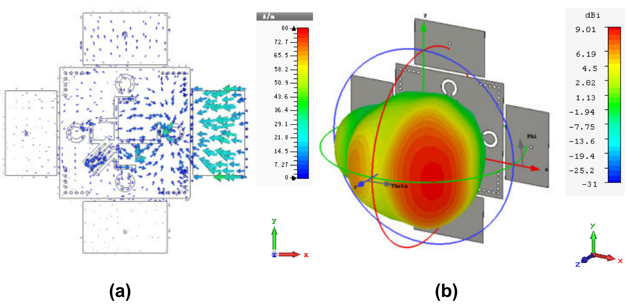

FIGURE 7. (a) Distribution of surface current and (b) Radiation pattern at 5.3GHz when port 1 is excited.

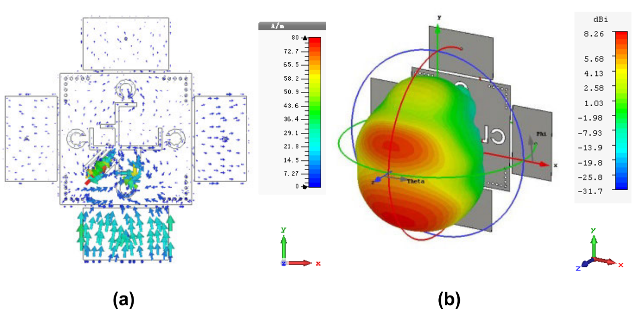

FIGURE 8. (a) Distribution of surface current and (b) Radiation pattern at 5.3GHz when port 4 is excited.

B. INFLUENCE OF THE ISOLATION GAP

In order to improve isolation between ports, an asymmetric gap is etched in the square patch. It is a resonator and forms a stop band at its resonant frequency. As a result, it will prevent surface current passing from one port to another. The resonant frequency of the isolation gap is determined by the dimensions of the gap. The results with and without gap are shown in Figure 9. It should be noted that the isolation gap can improve the isolation between all ports, especially S_{31}/S_{13}, which decreasing from -3 dB to less than -12 dB. In addition, when the port 1 and 3 is excited, the -10 dB impedance bandwidth are in the ranges of 5.05 - 5.49 GHz and 5.25 - 5.48 GHz, respectively. In two cases, the antenna can operate at 5.3 GHz and the overlapping band is from 5.25 to 5.48GHz. This indicates although the operating

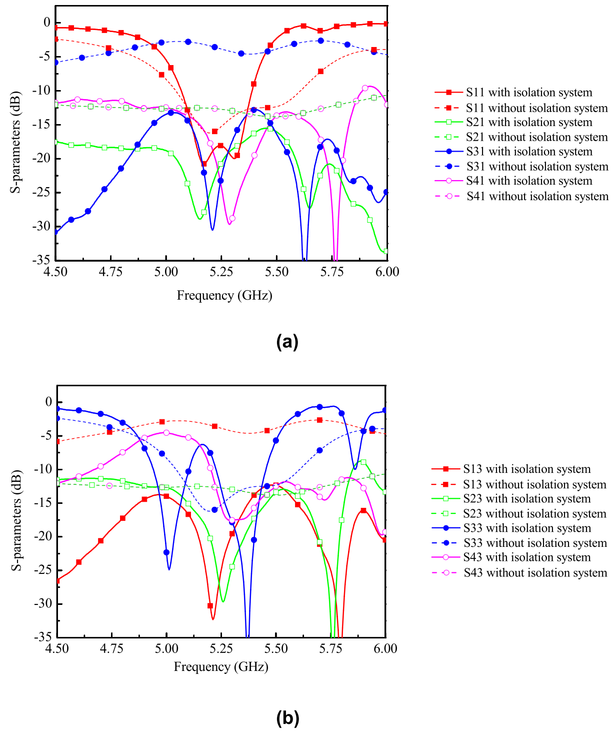

FIGURE 9. *S*-parameters with and without asymmetric gap (a) when port 1 is fed, (b) when port 3 is fed.

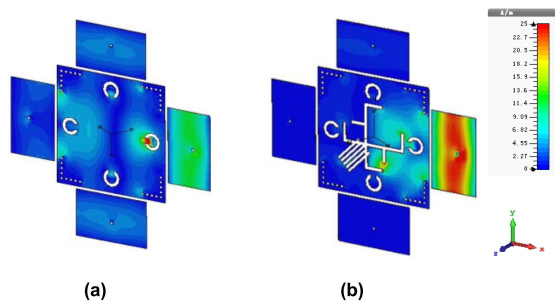

FIGURE 10. Surface current distribution at 5.3 GHz when port 1 is excited. (a) without isolation gap; (b) with isolation gap.

frequency range of port 1 is different from that of port 3, the antenna can work normally.

The improvement mechanism of isolation can be explained through the current distribution when port 1 is fed as shown in Figure 10. In Figure 10(a), before the asymmetric gap is arranged, some of current can flow to other ports, especially port 3. In case that the asymmetric gap appears, the current is basically limited near port 1 and that flowing to other ports is greatly reduced, as shown in Figure 10(b). Therefore, the isolation is improved. In case of port 3, a similar conclusion can be drawn as shown in Figure 11.

C. INFLUENCE OF THE OPEN RING

Finally, in order to further improve the impedance matching of multi-source multi-beam antenna, an open ring around each port is introduced. Here, we take S_{11}/S_{33} as an example to illustrate its influence and the results are shown

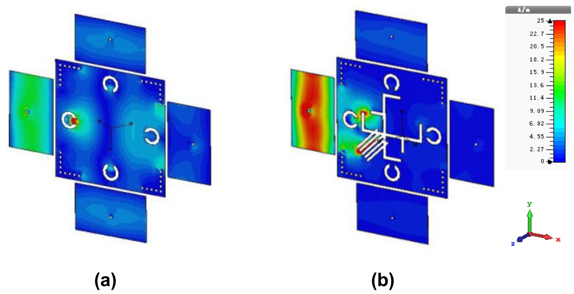

FIGURE 11. Surface current distribution at 5.3 GHz when port 3 is excited. (a) without isolation gap; (b) with isolation gap.

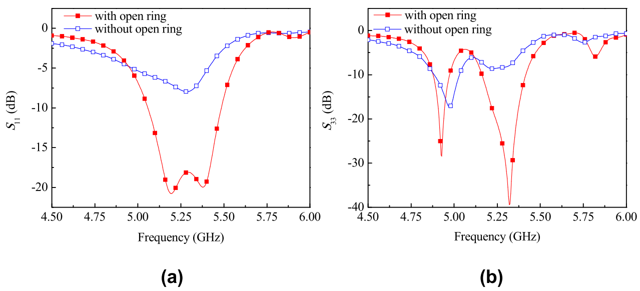

FIGURE 12. Effect of open ring on reflection coefficient (a) S_{11}, (b) S_{33}.

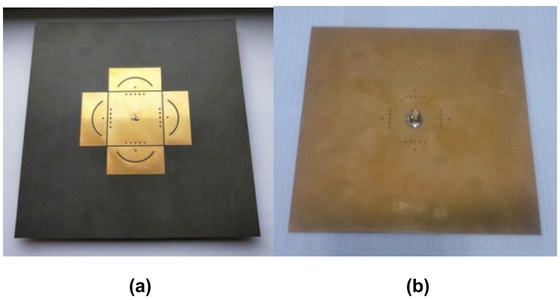

FIGURE 13. Photograph of the fabricated single-source multiple beam antenna. (a) Top view; (b) Bottom view.

in Figure 12. It indicates when an open ring is added, the impedance matching of the antenna in the working frequency band is improved significantly. For instance, at 5.3 GHz, S_{11} and S_{33} reduce to −18 and −30.5 dB from −8 and −8.3 dB, respectively. The reason that the opening ring can improve impedance matching is that new capacitance is introduced by it.

IV. SIMULATED AND MEASURED RESULTS

In order to verify the design method, single- and multi-source antennas are fabricated and measured. They are excited by SMA adaptors and measured using Agilent PNA network analyzer N5222A.

A. SINGLE-SOURCE MULTI-BEAM ANTENNA

Figure 13 shows the photograph of the fabricated single-source multi-beam antenna. The simulated and measured S_{11} and radiation patterns at 5.3 GHz are shown in Figures 14 and 15 respectively. It is clear from Figure 14 that the simulated and measured S_{11} match well except a little deterioration at the higher frequencies. The measured −10dB relative bandwidth is 3.8% (from 5.22 GHz to 5.42 GHz). In Figure 15, the simulated and measured radiation patterns are in good agreement. For the measured results, four beams are pointing to $(\varphi, \theta) = (0°, 41°)$, $(90°, 35°)$, $(180°, 41°)$

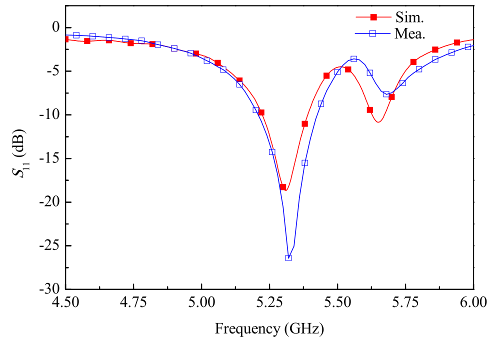

FIGURE 14. Simulated and measured S_{11} for single-source case.

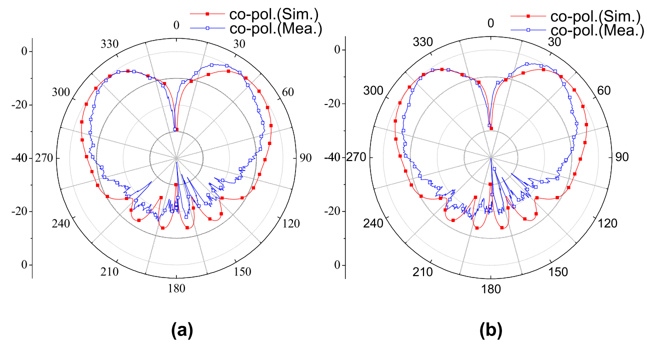

FIGURE 15. Simulated and measured normalized far-field radiation patterns in the (a) xz plane and (b) yz plane at 5.3 GHz.

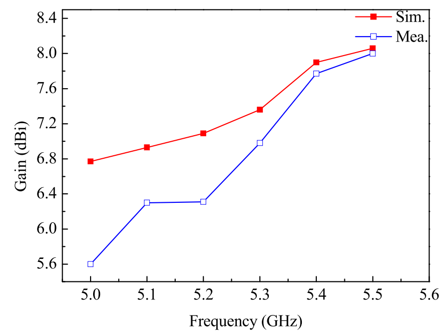

FIGURE 16. Realized gain for the single-source multi-beam antenna.

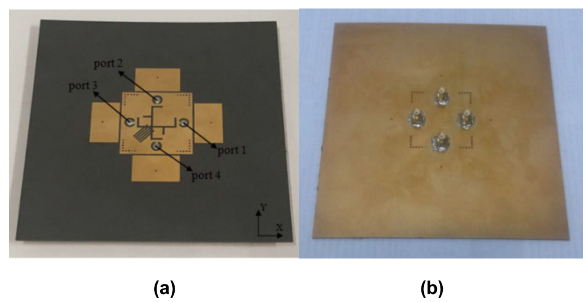

FIGURE 17. Photograph of the fabricated four sources multi-beam antenna. (a) Top view; (b) Bottom view.

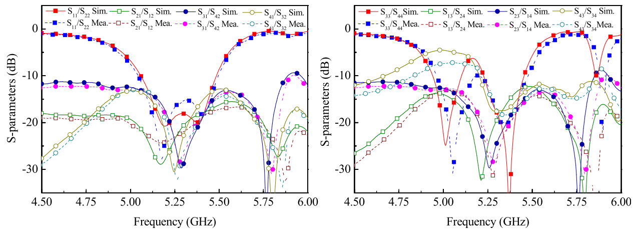

(a) (b)

FIGURE 18. **Simulated and measured *S*-parameters for (a) port 1/2; (b) port 3/4.**

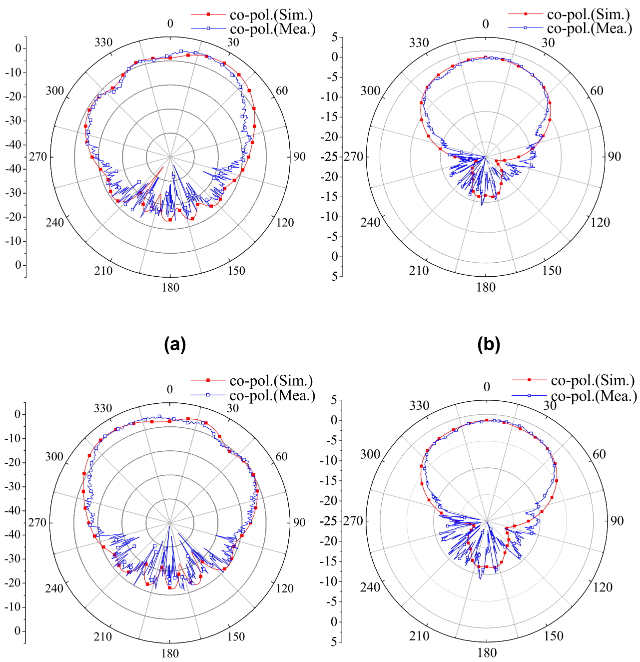

(a) (b) (c) (d)

FIGURE 19. **Simulated and measured far-field radiation patterns at 5.3 GHz. (a) port 1, E-plane; (b) port 1, H-plane; (c) port 4, E-plane; (d) port 4, H-plane.**

and (270°, 38°), which existing a slight distinction to the simulated one.

Finally, Figure 16 gives the realized gain of the fabricated single-source multi-beam antenna. The simulated and measured results are basically agreement and vary in the range of 7.09 - 7.90 dBi and 6.31 - 7.77 dBi, respectively.

B. MULTI-SOURCE MULTI-BEAM ANTENNA

The photograph of the fabricated multi-source multi-beam antenna is given in Figure 17 and measured results are shown in Figures 18-20. Figure 18 shows the simulated and measured *S*-parameters and they are in good agreement. In Figure 18(a), when port 1/2 is excited, the antenna can operate from 5.05 to 5.49 GHz. Isolation between excited port and other three ports is better than 12 dB within the entire operating frequency band, and the optimal value of 28 dB appears at 5.3 GHz. In case that port 3/4 is excited, the measured bandwidth of the proposed antenna is about 230 MHz (from 5.25 GHz to 5.48 GHz). In this band, the isolation between ports is better than 15 dB.

Figure 19 compares the simulated and measured far-field radiation pattern. Considering symmetry, we just need to clarify the results when ports 1 and 4 are excited. As can be seen, the simulation and measurement results are in good agreement. In Figures 19(a) and (b), when port 1 is excited, the main beam points at $(\varphi, \theta) = (0°, 30°)$. In Figures 19(c) and (d), when port 4 is excited, the main beam is steered at $(\varphi, \theta) = (270°, 37°)$. In addition, the case for ports 2 and 3 are also measured and the corresponding maximum radiation is located at $(\varphi, \theta) = (90°, 30°)$ and (180°, 37°), respectively.

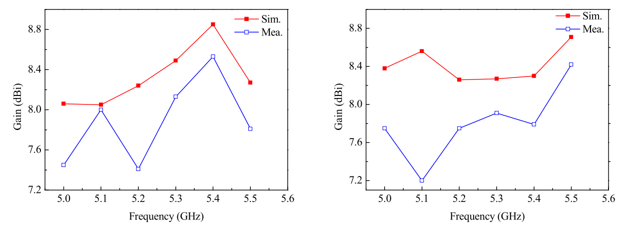

(a) (b)

FIGURE 20. **Realized gain for the multi-source multiple beam antenna. (a) port 1/2; (b) port 3/4.**

The realized gains of the proposed antenna with four ports are shown in Figure 20. When port 1/2 is excited, the simulated and measured maximum values of 8.85 and 8.53 dBi appear at 5.4 GHz. At the center frequency of 5.3GHz, the antenna has a gain of 8.13 dBi. For the case of port 3/4, the measured gain changes in range of 7.75-8.42 dBi, slightly less than the simulated one.

V. CONCLUSION

In this paper, one solution for designing multi-beam antennas is presented. It is based on parasitic patch and shorting-pin. Taking examples of both single- and multi- source cases, the working principle and measured results are presented. Also, the adjustment of the operating frequency of single-source antenna and improving isolation of multi-source case are provided. The simulated and measured results confirmed the solution. The realized single-source antenna operates in the range of 5.22 - 5.42 GHz and gain of four beams is about 6.98 dBi. For the multi-source case, the corresponding results are 5.25 - 5.48 GHz and 7.91 dBi. Compared to the normal multi-beam antenna, the presented antennas are compact, low-profile and suitable for various miniaturized communication systems.

REFERENCES

[1] S. Egami and M. Kawai, "An adaptive multiple beam system concept," *IEEE J. Sel. Areas Commun.*, vol. 5, no. 4, pp. 630–636, May 1987.

[2] M. Abdelghani, M. Niroo-Jazi, and T. Denidni, "Antenna beam shaping and gain enhancement using compensated phase conformal artificial magnetic reflector," *Microw. Opt. Technol. Lett.*, vol. 59, no. 4, pp. 880–883, Apr. 2017.

[3] A. Hosseini, S. Kabiri, and F. De Flaviis, "V-band high-gain printed quasi-parabolic reflector antenna with beam-steering," *IEEE Trans. Antennas Propag.*, vol. 65, no. 4, pp. 1589–1598, Apr. 2017.
[4] N. Llombart, A. Neto, G. Gerini, M. Bonnedal, and P. De Maagt, "Leaky wave enhanced feed arrays for the improvement of the edge of coverage gain in multibeam reflector antennas," *IEEE Trans. Antennas Propag.*, vol. 56, no. 5, pp. 1280–1291, May 2008.
[5] K. Wincza, K. Staszek, and S. Gruszczynski, "Broadband multibeam antenna arrays fed by frequency-dependent butler matrices," *IEEE Trans. Antennas Propag.*, vol. 65, no. 9, pp. 4539–4547, Sep. 2017.
[6] S. Gruszczynski, K. Wincza, and K. Sachse, "Reduced sidelobe four-beam N-element antenna arrays fed by 4$timesN$ butler matrices," *IEEE Antennas Wireless Propag. Lett.*, vol. 5, pp. 430–434, 2006.
[7] S. Mosca, F. Bilotti, A. Toscano, and L. Vegni, "A novel design method for Blass matrix beam-forming networks," *IEEE Trans. Antennas Propag.*, vol. 50, no. 2, pp. 225–232, Aug. 2002.
[8] Y. Li, X. Wan, B. Cai, Q. Cheng, and T. Cui, "Frequency-controls of electromagnetic multi-beam scanning by metasurfaces," *Sci. Rep.*, vol. 4, no. 1, Nov. 2014, Art. no. 6921.
[9] O. Yurduseven and D. R. Smith, "Dual-polarization printed holographic multibeam metasurface antenna," *IEEE Antennas Wireless Propag. Lett.*, vol. 16, pp. 2738–2741, 2017.
[10] H.-X. Xu, T. Cai, Y.-Q. Zhuang, Q. Peng, G.-M. Wang, and J.-G. Liang, "Dual-mode transmissive metasurface and its applications in multibeam transmitarray," *IEEE Trans. Antennas Propag.*, vol. 65, no. 4, pp. 1797–1806, Apr. 2017.
[11] S. Mohamad, A. Momeni, H. Abadi, and N. Behdad, "Wideband multi-beam antenna apertures using metamaterial-based superstrates," in *Proc. IEEE Antennas Propag. Soc. Int. Symp. (APSURSI)*, Memphis, TN, USA, Jul. 2014. pp. 926–927.
[12] D. Gonzalez-Ovejero, G. Minatti, G. Chattopadhyay, and S. Maci, "Multi-beam by metasurface antennas," *IEEE Trans. Antennas Propag.*, vol. 65, no. 6, pp. 2923–2930, Jun. 2017.
[13] D. Gonzalez-Ovejero, G. Minatti, E. Martini, G. Chattopadhyay, and S. Maci, "Shared aperture metasurface antennas for multibeam patterns," in *Proc. 11th Eur. Conf. Antennas Propag. (EUCAP)*, Paris, France, Mar. 2017., pp. 3332–3335.
[14] D. Gonzalez-Ovejero, G. Chattopadhyay, and S. Maci, "Multiple beam shared aperture modulated metasurface antennas," in *Proc. 2016 IEEE Int. Symp. Antennas Propag. (APSURSI)*, Fajardo, PR, USA, Jun./Jul. 2016, pp. 101–102.
[15] J.-S. Park, S.-H. Lee, and H.-K. Choi, "The characteristics of the dipole espar antenna using the cross-coplanar waveguide feed," *Microw. Opt. Technol. Lett.*, vol. 57, no. 10, pp. 2238–2242, Oct. 2015.
[16] Y. Myo Kyaw, J.-H. Oh, and H.-K. Choi, "Design of broadband double-curved cross dipole ESPAR antennas," *Microw. Opt. Technol. Lett.*, vol. 58, no. 8, pp. 1922–1926, Aug. 2016.
[17] D. Schaubert, F. Farrar, A. Sindoris, and S. Hayes, "Microstrip antennas with frequency agility and polarization diversity," *IEEE Trans. Antennas Propag.*, vol. 29, no. 1, pp. 118–123, Jan. 1981.
[18] X. Zhang and L. Zhu, "Gain-enhanced patch antennas with loading of shorting pins," *IEEE Trans. Antennas Propag.*, vol. 64, no. 8, pp. 3310–3318, Aug. 2016.

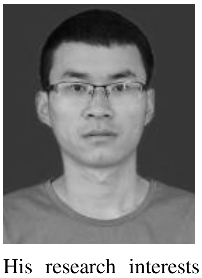

ZEKUI ZHANG received the B.Eng. degree in electronic information engineering from Northeastern University, Qinhuangdao, China, in 2012, and the M.A.Eng. degree in electronic and communication engineering from Sichuan University, Chengdu, China, in 2015. He is currently pursuing the Ph.D. degree in radio physics with Shanxi University, Taiyuan, China. He is also a Worker with the No.33 Research Institute of China Electronics Technology Group Corporation, Taiyuan. His research interests include multibeam antenna, high gain antenna, metasurface, and absorbing material.

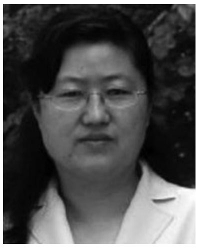

WENMEI ZHANG was born in 1969. She received the B.S. and M.S. degrees in electronic engineering from the Nanjing University of Science and Technology, Nanjing, China, in 1992 and 1995, respectively, and the Ph.D. degree in electronic engineering from Shanghai Jiao Tong University, Shanghai, China, in 2004. She is currently a Professor with the College of Physics and Electronics, Shanxi University, Taiyuan, China. Her research interests include microwave and millimeter-wave integrated circuits, EMC, and microstrip antenna.

YUFENG LIU received the Ph.D. degree in radio physics from Sichuan University, Sichuan, China, in 2014. In 2015, he joined the College of Physics and Electronic Engineering, Shanxi University. His research is mainly focused on computational electromagnetics and antenna design.

RUNBO MA was born in Shanxi Changzhi, China, in 1974. He received the B.S., M.S., and Ph.D. degrees from Shanxi University, Taiyuan, China, in 1993, 2002, and 2011, respectively, all in electronic engineering. He is currently an Associate Professor with the College of Physics and Electronics, Shanxi University. His research interests include microwave and millimeter-wave integrated circuits, RFID, and microstrip antenna.

LIPING HAN was born in Shanxi, Shuozhou, China, in 1970. She received the B.S., M.S., and Ph.D. degrees in electronic engineering from Shanxi University, Taiyuan, China, in 1993, 2002, and 2011, respectively. She is currently an Associate Professor with the College of Physics and Electronics, Shanxi University. Her research interests include microwave and millimeter-wave integrated circuits, and microstrip antenna.